

## Statistics of Coherent Groups in Three-Dimensional Fully-Nonlinear Potential Waves

E. V. Sanina<sup>1</sup>, S. A. Suslov<sup>1</sup>, D. Chalikov<sup>1,2</sup> and A. V. Babanin<sup>1</sup>

<sup>1</sup>Centre for Ocean Engineering, Science and Technology  
Swinburne University of Technology, Melbourne 3122, Australia

<sup>2</sup>Institute of Oceanography RAS  
Saint-Petersburg 199004, Russian Federation

### Abstract

We investigate the emergence of coherent groups in three-dimensional fully-nonlinear potential deep water waves whose initial spectrum is assumed to be of the JONSWAP type with directional distribution given by  $(\cos\theta)^n$ , where  $n$  is the integer varying from 1 to 16. The analysis is based on the results of long-term wave simulations performed using a numerical solution of a three-dimensional Laplace equation for the potential with nonlinear boundary conditions. The main characteristics of the wave groups such as average group velocity and maximum group wave height are analysed. The statistics of extreme wave occurrence in the groups are discussed.

### Introduction

The analysis of grouping properties of a wave field in space and time can be performed using various approaches. Traditionally, the wave elevation time series are acquired by in-situ sensors (i.e. anchored buoys, wave lasers) moored at a fixed position [2]. The alternative to the point measurements are remote sensing techniques capable of acquiring temporal sequences of images of the ocean surface. The mentioned methods have been used for the analysis of grouping features in many studies [7].

To detect coherent groups on the ocean surface obtained either from records or numerical simulations, the two-dimensional upper wave envelope (referred to as an envelope below) is constructed using various techniques: Riesz transform [5], Hilbert transform [3] or cubic spline approach described below.

### Numerical Model of Three-Dimensional Fully Nonlinear Potential Periodic Waves

We solve numerically the three-dimensional Laplace equation of the velocity potential  $\phi(x, y, z, t)$

$$\frac{\partial^2 \phi}{\partial x^2} + \frac{\partial^2 \phi}{\partial y^2} + \frac{\partial^2 \phi}{\partial z^2} = 0 \quad (1)$$

with the following boundary conditions at the free surface  $z = \eta(x, y, t)$ : kinematic condition

$$\frac{\partial \eta}{\partial t} + \frac{\partial \eta}{\partial x} \frac{\partial \phi}{\partial x} + \frac{\partial \eta}{\partial y} \frac{\partial \phi}{\partial y} - \frac{\partial \phi}{\partial z} = 0, \quad (2)$$

Bernoulli integral

$$\frac{\partial \phi}{\partial t} + \frac{1}{2} \left( \frac{\partial^2 \phi}{\partial x^2} + \frac{\partial^2 \phi}{\partial y^2} + \frac{\partial^2 \phi}{\partial z^2} \right) + \eta = 0, \quad (3)$$

and  $\frac{\partial \phi}{\partial z} = 0$  at  $z \rightarrow -\infty$ , where  $(x, y, z)$  are the Cartesian coordinates and  $t$  is time. The equations are solved in the infinite domain bounded by the wave surface:  $-\infty < x < \infty$ ,  $-\infty < y < \infty$ ,

$-\infty < z \leq \eta(x, y, t)$ . The variables  $\phi$  and  $\eta$  are considered to be periodic in the  $x$  and  $y$  directions.

The numerical solution introduced in [1] is obtained in the non-stationary surface-following non-orthogonal coordinate system

$$\xi = x, \quad \nu = y, \quad \zeta = z - \eta(\xi, \nu, t). \quad (4)$$

The equations in the new coordinates are Fourier-transformed in the horizontal directions and are discretised using central differences in the vertical direction. The obtained system of ordinary differential equations for Fourier coefficients is integrated in time using the 4th order Runge-Kutta method.

### Detection of Wave Groups

#### Construction of a One-Dimensional Wave Envelope

We define an envelope of a unidirectional wave using a cubic interpolation connecting local maxima of a wave surface. The wave group is then identified to be between the two envelope minima as shown by thick dashed line in figure 1.

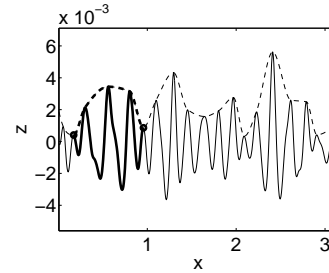


Figure 1: Constructing one-dimensional wave (solid line) upper envelope using the directional cubic spline (dashed line). The thick line shows the detected group.

#### Detection of Groups in a Two-Dimensional Wave Field

In order to define the upper envelope on the two-dimensional ocean surface we consider its sections forming angle  $\theta$  with the main wave propagation direction. The range for the angles is  $-90^\circ \leq \theta \leq 90^\circ$ . Since the surface elevation is computed at discrete grid points only the values nearest to the section plane are considered without any interpolation. The  $y$  distance between the sections is chosen to be  $\frac{2\pi}{256}$ . For the directional sections the periodicity of the computed fields in the  $Oy$  direction is used.

The one-dimensional groups detected in the sections are combined into two-dimensional groups as described below. Two one-dimensional groups in the neighbouring sections found for the angle  $\theta$  are combined if the distance between these one-dimensional sections  $d_1$  is smaller than a half of the peak wavelength  $\lambda_p$  and the distance between the middle points of the

groups in the direction of the sections is  $d_2 \leq \frac{1}{4}l_{min}$ , where  $l_{min}$  is the minimum length of the one-dimensional group defined as  $l_{min} = 4\lambda_p$ , where  $\lambda_p$  is the main wave length. The described distances are shown in figure 2 a). The two-dimensional wave group is defined as an embedding rectangle containing the combined one-dimensional groups as shown in figure 2 b).

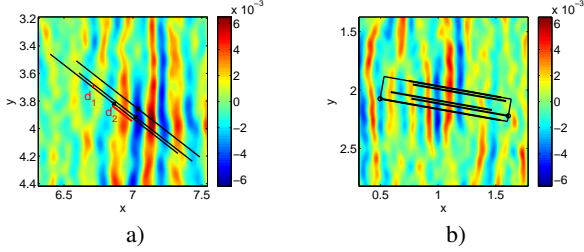


Figure 2: a) Group detection parameters, b) the rectangle embedding combined one-dimensional groups.

The characteristics of the detected groups such as their velocity and maximum height are investigated as the properties of the subsurface in the embedding rectangles. The example of such a subsurface is shown in figure 3.

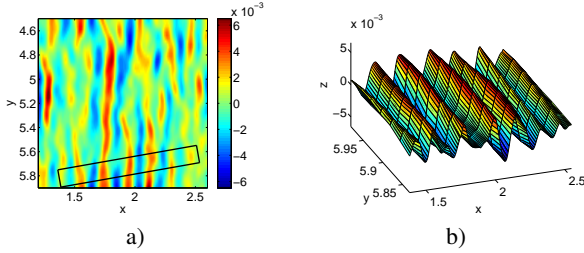


Figure 3: Subsurface corresponding to the detected group rectangle: a) group position on the surface, b) three-dimensional view of the group surface.

#### Detection of Group Tracks in a Two-Dimensional Wave Field

We define group track as a sequence of embedding rectangles introduced for sequential time steps. We consider the consecutive snapshots of the two-dimensional wave field taken with the time intervals  $\Delta t \approx 0.45T_p$  and the group rectangle corresponding to each of the snapshots in the track sequence. When analysing a wave field we consider all group rectangles detected in the  $\theta$  direction and intersected by a line specifying this direction. We define the width  $w$  of the group as the number of sections in the  $y$  direction, with the distance of  $\frac{2\pi}{256}$  between them, that intersect the embedding rectangle. A "wide" group is detected if:  $k > 4$ , where  $k$  is the number of the detected one-dimensional groups in the rectangle, and  $w - k < k$ , so that there are no large distances between the one-dimensional groups. The example of a "wide" group is shown in figure 2 b).

Subsequently, we distinguish two situations. If there are "wide" groups along the chosen direction, we first combine them in the sequence. The individual groups detected for the moments  $t_1$  and  $t_2$  in time are only combined if  $t_2 - t_1 < 5T_p$ , where  $T_p$  is the wave peak period. Then for each sequence we define its width and position as those of a stripe containing all wide groups between the dashed lines in figure 4 a)). Additionally, we combine the groups found in the same snapshots by embedding them into bigger rectangles if  $d \leq 0.8l_{min}$ , where  $d$  is the distance between the centers of the rectangles. If only narrow groups are present we choose only those of them that are intersected by the chosen direction line as shown in figure 4 b).

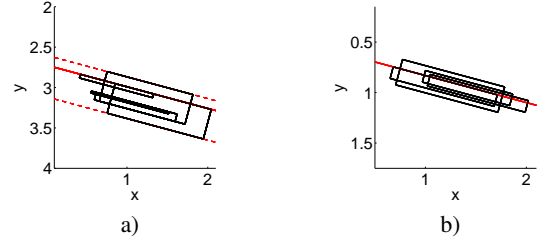


Figure 4: Track detection along a line in the chosen direction with: a) wide groups, b) only narrow groups.

The two groups belonging to different snapshots are combined in a track if the distance  $d$  between centers of the respective embedding rectangles is smaller than  $\frac{4}{5}\lambda_p$  if the center moves in the main wave propagation direction or smaller than  $\frac{1}{4}\lambda_p$ , if the center moves in the opposite direction (due to the elongation of the embedding rectangle). If more than one group is chosen from the same snapshot, the group with the minimal  $d$  from the previous snapshot is added to the track.

Note that the same track can be identified along two or more nearby sections. Thus to avoid double counting we only consider the longest detected track and ignore other shorter tracks that contain the same groups.

#### Filtering Group Tracks Found for Different Directions

As can be seen from figure 5, the same group and track can be identified for different directions  $\theta$ . To filter out the tracks detected more than once for the range of  $\theta$  the following method is used.

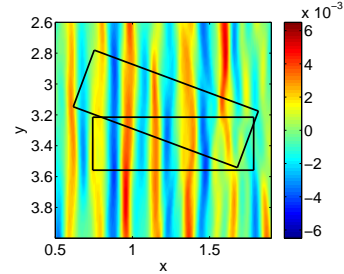


Figure 5: A wide group detected in both directions  $\theta = 0^\circ$  and  $\theta = 25^\circ$  in the wave field with the initial directionality index  $n = 16$ .

We find all pairs of groups from the tracks that correspond to the same time for which the overlap of their embedding rectangles is larger than 0.5 of the area of at least one of the rectangles in the pair. Then we combine the tracks that have more than 1 of such common groups. Subsequently, we filter tracks using the following maximum steepness criterion.

The track steepness is defined as the maximum steepness  $\epsilon_g$  of the group subsurfaces that it consists of:

$$\epsilon_g = \frac{H_s^{sub}}{2} k_p^{sub} \frac{2\pi}{L^{sub}}, \quad (5)$$

where  $H_s^{sub}$  is the significant waveheight of the subsurface, which is four times the standard deviation of the subsurface elevation field from the mean value,  $k_p^{sub}$  is the peak wavenumber of the subsurface and  $L^{sub}$  is the length of the subsurface.

Statistics of the average group velocity and the maximum wave height of the filtered and unfiltered results were compared and found identical. Thus filtering influences only the number of tracks analysed.

### Group Analysis Results for Two-Dimensional Wave Fields

We analyse wave fields with different directionality indices ( $n = 1, 2, 4, 16$ ) in the directions  $\theta = -45^\circ \dots 45^\circ$  with the step  $\Delta\theta = 1^\circ$ . The calculations were made for the time interval of 135 peak wave periods starting from about the 67th wave period of the calculations. The groups were detected on the 1/3 part of the simulated wave field (rectangle  $\frac{1}{3}2\pi\cos(\theta) \times 2\pi$  with the periodicity in the  $Oy$  direction to cover the same length of the field in all directions  $\theta$ ). The summary of the group statistics analysis is given in table 1.

$n$	$N$	$v_g$	$std(v_g)$	$H_s$	$\frac{H_g}{H_s}$	$std(\frac{H_g}{H_s})$
1	1184	0.13	0.05	0.0062	1.5	0.2
2	2255			0.0069	1.4	
4	2028			0.0072	1.3	
16	938			0.0073	1.2	

Table 1: Wave groups statistics. The number of groups  $N$ , the group velocities  $v_g$ , the significant wave heights  $H_s$ , the group wave heights  $H_g$  normalised with  $H_s$  and their standard deviations.

### The Number of Groups

The total number of the detected tracks increases from 1184 for  $n = 1$  to 2255 for  $n = 2$  (see Tab. 1, column  $N$ ). With the further increase of  $n$  the number of the detected tracks decreases as the wave fields become narrowly directed. The directional distributions of the detected number of tracks filtered using the maximum steepness criterion are shown in figure 6 a) by solid lines for several values of the initial spectrum directionality index. The corresponding fourth order polynomial least square regressions are shown by the dashed lines. For the directionality index  $n = 1$  the number of tracks decreases with the increase of  $|\theta|$ . As  $n$  increases the groups become wider and are found to propagate in the directions with larger angles  $\theta$ . This is illustrated in figure 5 where two groups detected for angles  $\theta = 0^\circ$  and  $\theta = 25^\circ$  are shown at the same location. The wave field contains wide enough groups so that the same group will be detected as moving in both inspected directions. It is highlighted by fourth order polynomial regressions of the distributions (dashed lines) normalised by the value at  $\theta = 0^\circ$  in figure 6 b). The average lifetime of the detected groups is  $1.6T_p$ .

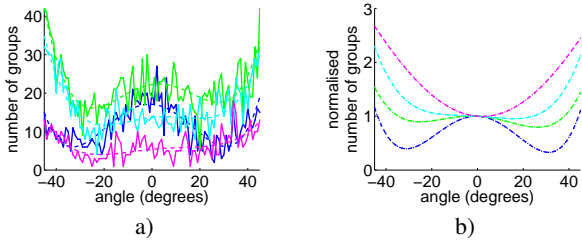


Figure 6: a) Directional distribution of the number of detected groups in the wave fields with the initial directionality indices  $n = 1, 2, 4, 16$  (blue, green, cyan and magenta lines, respectively) (solid lines) and their fourth order polynomial regressions (dashed lines). b) The same directional distributions normalised by the values for the main wave propagation direction  $\theta = 0^\circ$ .

### Velocity of Groups

The velocity of groups in wave systems has been investigated in many studies [6, 4] using numerical simulations and experimental radar measurements. Different approaches have been used for its calculation. For example in [6] the speed of propagation of the surface envelope was investigated using spectral methods and it was found to be 40% of the phase velocity at the spectral maximum.

The group velocity in the linear theory of gravity waves is defined as  $c_g = \frac{1}{2}\sqrt{\frac{g}{k_p}}$ , where  $g$  is the gravity and  $k_p$  is the wavenumber of the spectrum peak. In the non-dimensional field the theoretical group velocity then is  $c_g \approx 0.09$  for  $k_p = 32$ . The perceived velocity  $v_g$  of the detected groups is found as the velocity of the centers of embedding rectangles. The average value for the detected groups is  $v_g \approx 0.13$ , which is 44% larger than a theoretical group velocity.

The average velocities of the groups as well as their standard deviations are found to be similar for fields with all initial directionality indices  $n$ . The values are summarised in table 1. The behavior of the mean values of velocities of the groups  $v_g$  and their standard deviations with the increase of  $n$  is shown in figure 7.

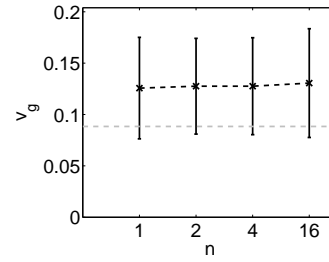


Figure 7: The average velocities of groups  $v_g$  and their standard deviations for various initial directionality indices. The group velocity in the linear gravity wave theory  $c_g$  is shown with the grey dashed line.

In figure 8 the directional distributions of the average velocities of groups are shown for various directionality indices  $n = 1, 2, 4, 16$ . As seen from the figure, the average velocity of groups propagating in different directions is virtually independent of the direction, except for  $n = 16$  where there is a small increase of the average velocity for  $-10^\circ < \theta < 10^\circ$ .

### Maximum Wave Height

In order to analyse the occurrence of the extreme waves we calculate the maximum wave heights in the detected groups. We apply zero-crossing analysis for sections along the wave group and find the maximum of the individual wave heights  $H_g$ . To compare the results for wave fields with different directionality indices we normalise  $H_g$  relative to the significant wave height for the wave field (mean value of the time series). The  $H_s$  values are given in table 1.

It can be seen from figure 9 a) and table 1 that the normalised group heights averaged over the detected groups decrease from 1.5 for  $n = 1$  to 1.2 for  $n = 16$ . The wider the initial spectra are the more likely a high wave is to be observed. Specifically, we found that the probability of observing a rogue wave is 2.6% for  $n = 1$  and 1% for  $n = 2$ . No extreme waves have been found in the detected groups for  $n = 4$  and  $n = 16$ .

The diagrams in figure 10 show the values of  $H_g/H_s$  for groups

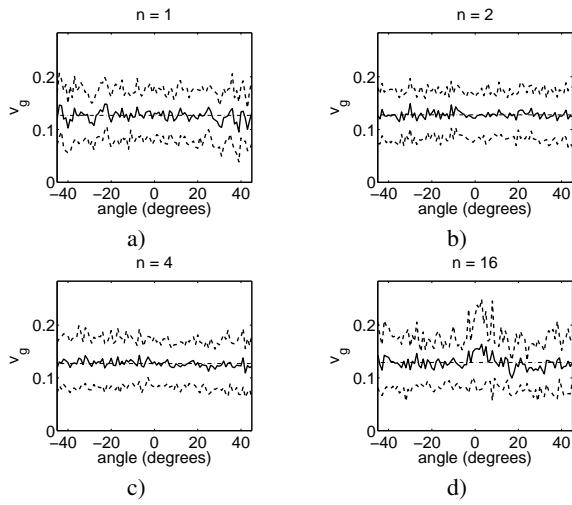


Figure 8: Directional distribution of the average velocity of groups  $v_g$  (solid line) and its standard deviation (dashed line) in the wave fields with the initial directionality index a)  $n = 1$ , b)  $n = 2$ , c)  $n = 4$ , d)  $n = 16$ .

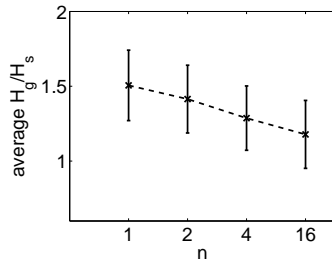


Figure 9: The average maximum wave height for initial directionality indices  $n = 1, 2, 4, 16$ .

detected in the direction angle interval  $-45^\circ \leq \theta \leq 45^\circ$ . The groups containing extreme waves are shown by red circles. For  $n = 1$  and  $n = 2$  the extreme wave cases are more likely to occur in the main propagation direction. The statistics of the average  $H_g/H_s$  values and their standard deviation are constant for all directions (see the solid line for the average value and the dashed line for the standard deviation).

## Conclusions

The statistics of the wave groups is analysed for the three-dimensional wave fields with the initial directionality indices  $n = 1, 2, 4, 16$  in the directions  $\theta = -45^\circ \dots 45^\circ$ . Wave groups are detected by considering envelopes of unidirectional wave constructed using the cubic interpolation connecting local maxima of a surface, and combining them into two-dimensional groups. The total number of the detected wave groups increases with the growth of  $n = 1$  to  $n = 2$  and then decreases with the further growth of  $n$  that narrows of the wave field spectrum. The average value of the perceived velocity of the detected groups  $v_g$  is found constant for all  $n$  in all directions  $\theta$ . The average value of the maximum wave heights in the groups normalised with significant wave height for the wave field is found to be decreasing with the increase of  $n$ . The high waves or rogue waves are found more likely to be observed in the fields with the wider initial spectra and in the main propagation direction.

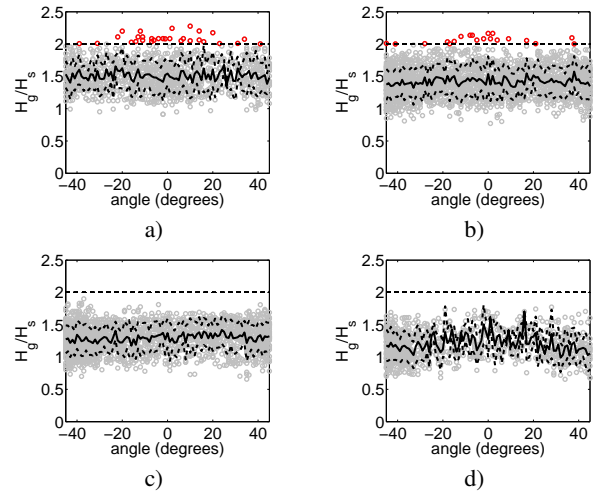


Figure 10: Directional distribution of the average maximum group wave height (solid line) and its standard deviation (dashed line) for the initial directionality indices a)  $n = 1$ , b)  $n = 2$ , c)  $n = 4$ , d)  $n = 16$ .

## Acknowledgements

The numerical simulations were performed at Swinburne University of Technology's supercomputer facility "Green machine".

## References

- [1] Chalikov, D. and Babanin, A. V., Three-dimensional periodic fully nonlinear potential waves, *ASME 2013 32nd International Conference on Ocean, Offshore and Arctic Engineering*, V02BT02A056.
- [2] Hamilton, J., Hui, W. H. and Donelan, M. A., A statistical model for groupiness in wind waves, *J. Geophys. Res. Oceans*, **84**, 1979, 4875–4884.
- [3] Huang, N. E., Shen, Z. and Long, S. R., A new view of nonlinear water waves: The hilbert spectrum, *Annu. Rev. of Fluid Mech.*, **31**, 1999, 417–457.
- [4] McKenzie, J. F., The group velocity and radiation pattern of rossby waves, *Geophys. Astrophys. Fluid Dyn.*.
- [5] Rice, S. O., Mathematical analysis of random noise, *Bell Syst. Tech. J.*, **23**, 1944, 282–332.
- [6] Yefimov, V. V. and Babanin, A. V., Dispersion relation for the envelope of groups of wind waves, *Izv. Atmos. Oceanic Phys.*, **27**, 1991, 599–603.
- [7] Ziemer, F. and Dittmer, J., A system to monitor ocean wave fields, *OCEANS '94. 'Oceans Engineering for Today's Technology and Tomorrow's Preservation.'* *Proceedings*, **2**, 1994, II/28–II/31 vol.2.